Journal of Materials Chemistry A

Accepted Manuscript

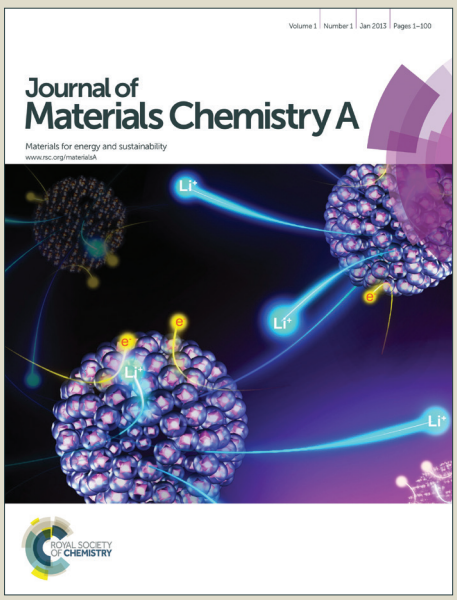

ROYAL SOCIETY OF CHEMISTRY

www.rsc.org/materialsA

Thermo-Responsive and Fluorescent Cellulose Nanocrystals Grafted with Polymer Brushes

Weibing Wu,[ab] Fang Huang,[b] Shaobo Pan,[b] Wei Mu,[b] Xianzhi Meng,[b] Haitao Yang,[c] Zhaoyang Xu,[d] Arthur J. Ragauskas[b] and Yulin Deng*[b]

Received (in XXX, XXX) Xth XXXXXXXXX 20XX, Accepted Xth XXXXXXXXX 20XX

DOI: 10.1039/b000000x

Cellulose nanocrystals (CNCs) grafted with fluorescent and thermo-responsive poly (*N*-isopropylacryalamide) (PNIPAAM) brushes were prepared via surface-initiated activators generated by electron transfer for atom transfer radical polymerization (SI-AGET-ATRP) in CH_3OH/H_2O mixing solvent with different volume ratios. The successful grafting was supported by Fourier transform infrared (FTIR) and nuclear magnetic resonance (NMR) measurements. Gravimetric analysis plus ^1H NMR and gel permeation chromatography (GPC) measurements showed that there was an increase in the monomer conversion and molecular weight of polymer brushes with increasing H_2O proportion of the solvent system. The variation trend of graft length was further evidenced by the gradual change of decomposition and glass transition temperatures of the surface-grafted CNCs. A large scale of chain transfer occurred on the surface of CNCs in view of the minute quantity of free polymers generated by sacrificial initiator.

Free polymers cannot be used as substitute to characterize grafted polymers in terms of the big difference between their molecular weights. The obtained surface-grafted CNCs showed thermo-enhanced fluorescence owing to the thermal-driven chain dehydration of the grafted PNIPAAM brushes.

Introduction

Stimuli-responsive nanomaterials have attracted significant attention over the last decade, finding applications in the fields of sensors, drug delivery, nanomedicine and environmental monitoring.[1-3] Among the various nanomaterials that have been modified to possess sensing capabilities, cellulose nanocrystals (CNCs) have received little attention in this regard. [4] CNCs, typically produced after acid hydrolysis of the amorphous regions of native cellulose, are rod-like particles with size of 50-300 nm in length and 3-20 nm in width. [5,6] Besides abundance, low cost, renewability and biodegradability, CNCs also possess high specific surface area and a large number of reactive hydroxyl groups on the surface that facilitate the modification with chemical species and fabrication of topology structure along the crystalline backbone. [7,8] Previously reported surface modifications included sulfonation, esterification,[9] oxidation,[10] cationization,[11] silylation,[12] and grafting.[13-16] One way to obtain stimuli-responsive CNCs is the attachment of analyte-sensitive small molecules or macromolecules onto hydroxyl groups. pH-Sensing CNCs have been prepared by dual fluorescent labeling with sensitive fluorophores.[17] There are also some other previous

studies focusing on the methods of dye labeling on CNCs and other related applications.[18-21] Attachment of macromolecules is a modular "grafting-to" approach in which the presynthesized polymers are fully characterized and purified before attaching to cellulose substrate. Much effort has been made to attach responsive polymers to the surface of CNCs via "grafting-to" method. [22-25,] Thermo-sensitive amine-terminated statistical polymers (Jeffamines) were grafted onto CNCs via a peptidic coupling reaction, leading to unusual properties like colloidal stability at high ionic strength and thermo-reversible aggregation. [23] The grafting of single-stranded oligonucleotides to CNCs has also resulted in responsive, self-assembling nanostructures that can be disassembled by increasing the temperature above the melting point of duplexed DNA. [24] However, the biggest challenge of "grafting-to" technique is the low grafting density due to its steric hindrance.[22] Another widely used synthetic strategy to yield sensing CNCs is grafting responsive polymer brushes from cellulose backbone. Higher grafting densities can be obtained by using this "grafting-from" method, while polymer brushes are formed by *in-situ* polymerization from surface-immobilized initiators. Alternatively, other functional groups could be introduced into the polymer brushes via copolymerization using this synthetic strategy as well. Previous reports of stimuli-responsive polymer brushes attached to CNCs via "grafting-from" approach are relatively scarce, including thermo-responsive poly(*N*-isopropylacrylamine),[26-28] theromo-responsive

poly(*N*,*N*-dimethylaminoethyl methacrylate),[29] and pH-responsive poly(4-vinylpyridine).[30]

Atom transfer radical polymerization (ATRP), one of the most successful "controlled/living" radical polymerizations developed during recent years, has been used extensively as a tool for the development of novel macromolecular structures.[31,32] The direct introduction of haloesters to the surface of inorganic or organic materials, as ATRP initiators, via esterification reactions makes surface-initiated ATRP (SI-ATRP) an efficient way to fabricate hybrids attached with polymer chains or brushes exhibiting high surface grafting density and low polydispersity via "grafting-from" strategy.[33] Many recent efforts in polymer-grafted CNCs via SI-ATRP have been reported in literature. [26,29,34-37,] To our best knowledge, no particular studies have focused on fluorescent and thermo-responsive nanomaterials based on polymer-grafted CNCs. Here we present a versatile synthetic strategy to fabricate CNCs grafted with fluorescent and thermo-responsive polymer brushes via surface-initiated activators generated by electron transfer for atom transfer radical polymerization (SI-AGET-ATRP)). The utilization of AGET-ATRP provides all the benefits of a normal ATRP process as well as the additional benefits of tolerance of the existence of a small amount of oxygen since it uses an electron transfer rather than organic radicals to reduce the higher oxidation state of the transition metal.[38] Poly(*N*-isopropylacrylamine) (PNIPAAM), which exhibits a soluble-to-insoluble change in aqueous solution in response to temperature around its

lower critical solution temperature (LCST) of 32 ^{o}C [39,40] was selected as the basic structure of the polymer grafts. A polymerizable fluorescent dye 4-ethoxy-9-allyl-1,8-naphthalimide (EANI) [41,42] with excellent fluorescent properties was covalently encapsulated into the PNIPAAM side chains via copolymerization. This study also addressed the important issue of grafting PNIPAAM from CNCs to develop brushes under various solvent conditions. This promising synthetic strategy provides potential opportunities to fabricate CNCs-based sensing nanomaterials that may benefit from multi-functionalities.

Experimental

Materials

The fully bleached softwood kraft pulp used to prepare CNCs is commercially available. 2-Bromoisobutyryl bromide (BiB, 98%), ethyl α-bromoisobutyrate (EBiB, 98%), 4-bromo-1,8-naphthalic anhydride (95%), 2-dimethylaminopyridine (DMAP, 99%), allylamine (99%), copper(II) bromide ($CuBr_2$, 99%), L-ascorbic acid (AsAc, 99%) and *N,N,N′,N″,N″*- pentamethyldiethylenetriamine (PMDETA, 99%), 1-methyl-2-pyrrolidinone (99.5%), sulfuric acid (95~98%), tetrahydrofuran (THF, 99.9%), acetone (99.8%), ethanol (99.5%), and methanol (CH_3OH, 99.8%) were all purchased from Sigma-Aldrich. *N*-isopropylacryalamide (NIPAAM, 97%), hexane (95%), triethylamine (TEA, 99.5%), anhydrous dimethylformamide (DMF, 99.8%),

sodium hydroxide solution (50% in water) were purchased from VWR. NIPAAM was recrystallized from hexane and dried under vacuum prior to use. 4-ethoxy-9-allyl-1, 8-naphthalimide (EANI) was synthesized according to literature (See Supporting Information).[42] All other chemicals were used as received without any further purification.

Preparation of Cellulose Nanocrystals

CNCs were prepared following a published method utilizing sulfuric acid.[43] In brief, softwood kraft pulp without any treatment was ground in a Wiley Mini-Mill to pass through a 20-mesh screen. The milled powder (50.0 g) was treated under stirring with a mechanical stirrer with 500 mL of 64 wt% H_2SO_4 at 45 ^oC for 45 min. The hydrolysis was then halted by adding 10-fold dilution of deionized (DI) water. The sediment was centrifuged for 10 min at 5,000 rpm under cooling condition (4 ^oC) and redispersed in DI water after discarding of the supernatant. Then the product was dialyzed against DI water for 7 days using the regenerated cellulose dialysis tubing with a 12,000~14,000 molecular weight cut off until the pH of the dialysis water stayed constant. Sonication using a Branson Sonifier was performed to the neutral whiskers solution for 30 min while sitting in an ice bath. The colloidal suspension was centrifuged for 5 min at 5,000 rpm and the cloudy supernatant was collected. This entire process was repeated multiple times until the supernatant became clear. The collected supernatant was then treated with

mixed bed ion exchange resin (TMD-8 hydrogen and hydroxide form) and kept at 5 ^{o}C. CNC powder was recovered by freeze-drying prior to use.

Immobilization of Initiator on CNCs

The dried CNCs (~1.5 g) was rinsed in 120 mL DMF and subsequently ultrasonicated under ice-bath cooling for 15 min prior to initiator immobilization. After the addition of DMAP (0.8 g, 6.6 mmol) and TEA (6.7 g, 66 mmol), the CNC suspension was heated to 70 ^{o}C under stirring. Then BiB (14.3 g, 64 mmol) dissolved in 30 mL DMF was added dropwise to the mixture within 0.5 h under a nitrogen atmosphere. The reaction was allowed to proceed with stirring at 70 ^{o}C for 24 h. The resulted esterified CNCs was subsequently washed with THF, acetone and methanol via redispersion under sonication and centrifugation at 12, 000 rpm for 20 min under cooling condition (4 ^{o}C) to remove any residuals. The purified product was redispersed under sonication and kept in methanol. Powder product was obtained by centrifuging and oven-drying under vacuum at 40 ^{o}C for 48 h.

Grafting of Polymer Brushes from Initiator-Immobilized CNCs

The initiator-immobilized CNCs (CNC-Br) were grafted with Poly(NIPAAM-*co*-EANI)

by AGET-ATRP in the two-component solvent system of CH_3OH/H_2O with different volume ratios. CNC-G1, CNC-G2, CNC-G3, CNC-G4 and CNC-G5 were referred to the volume ratios of 1:0, 4:1, 2:1, 1:1 and 1:2, respectively. The polymerization was conducted in the presence of both CNC-Br and EBiB (sacrificial initiator) with the initial monomer concentration ($[M]_0$) of 2 M. The typical procedure is shown as follows: To a Schlenk tube fitted with a magnetic stir bar and a rubber septum, NIPAAM (4.52 g, 40.0 mmol), EANI (112 mg, 0.4 mmol), CNC-Br (200 mg), EBiB (39 mg, 0.2 mmol), $CuBr_2$ (89 mg, 0.4 mmol), PMDETA (166 μL, 0.8 mmol), and CH_3OH /H_2O mixture (15 mL, designed volume ratio) were charged and the mixture was bubbled with nitrogen for 20 min. At the same time, to another vial fitted with a magnetic stir bar and a rubber septum, AsAc (35 mg, 0.2 mmol) and CH_3OH /H_2O mixture (5 mL, designed volume ratio) was charged and the solution was bubbled with nitrogen for 15 min as well . Afterwards, the degassed AsAc solution was transferred via cannula to the first Schlenk tube. The Schlenk tube was sealed and the mixed solution was allowed to polymerize at ambient temperature (~21 ^oC) for 8 h. Then the reaction mixture was exposed to air to quench the polymerization. The reaction mixture was centrifuged for 20 min at 12,000 rpm under 4 ^oC. The collected supernatant was diluted with D_2O for ^1H NMR analysis or filtered through a column of neutral alumina to remove the catalyst residues for GPC analysis. The isolated precipitates were purified by successive washing (the same as the washing process of CNC-Br) with acetone, DI water and methanol until no absorption at 375 nm

of EANI in the supernatant was detected. The resulted surface-grafted CNCs were redispersed under sonication and kept in DI water. Part of them was recovered by freeze-drying prior to analysis. Scheme 1 shows a summary of the key steps involved in the production of surface-grafted CNCs.

Scheme 1 Synthesis Route for the Immobilization of Initiator on CNCs and Subsequent Surface Grafting of Poly(NIPAAM-*co*-EANI)

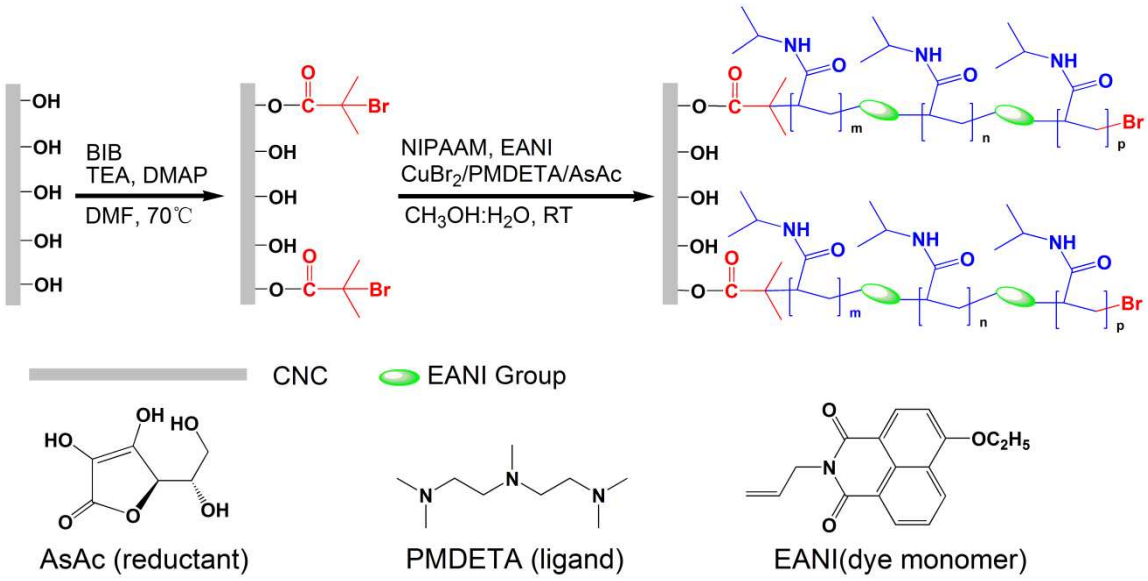

Cleavage of Polymer Brushes from Surface-Grafted CNCs

In order to characterize the grafted polymer brushes on CNCs, cleavage of grafts was conducted by saponification of surface-grafted CNCs. [26] 150 mg of surface-grafted CNC

was placed in 15 mL 2 wt% NaOH solution for 48 h while stirring at room temperature. Afterwards, the dispersion was neutralized with 1 M HCl and then centrifuged at 12,000 rpm for 20 min at 4 ^{o}C to separate CNCs from the suspension. The obtained CNCs were recovered by freeze-drying after successive washing by redispersion and centrifugation in DI water to remove residual polymers and salts. The supernatant containing cleaved polymer grafts was directly freeze-dried and the recovered product was rinsed in THF under stirring, centrifuged (12, 000 rpm for 20 min at 4 ^{o}C) and filtered through 0.45 um PET syringe filter prior to GPC analysis.

Fourier Transform Infrared (FTIR) Spectroscopy

FTIR spectra were recorded on a Perkin ElmerTM 100 Spectrometer with a universal ATR sampling accessory. Spectra were recorded between 650 and 4,000 cm^{-1} at a resolution of 4 cm^{-1} and 64 scans were collected for each spectrum. The ATR correction and the baseline correction were carried out orderly by PerkinElmer Spectrum software.

Transmission Electron Microscopy (TEM)

TEM images were acquired on a JEOL 100CX II transmission electron microscope using an acceleration voltage of 80 kV. The TEM samples were prepared by placing a drop of a diluted suspension of CNCs on a carbon coated grid followed by stain with 2 wt% uranyl acetate in water solution for 5 min and dried before analysis.

Nuclear Magnetic Resonance (NMR) Spectrometry

^{1}H NMR and solid-state ^{13}C NMR spectral data were recorded with a Bruker Avance/DMX 400 MHz NMR spectrometer at 25 ^{o}C. Solid-state ^{13}C NMR analysis was performed at a frequency of 100.59 MHz over 32 K data points with acquisition time 0.67 s using a gated 1 H decoupling sequence with a 1-s pulse delay and 10 K scans.

Gel Permeation Chromatography (GPC)

Both cleaved polymers from surface-grafted CNCs and free polymers generated by sacrificial initiator were characterized by SECcurity GPC System (Agilent Technologyies, 1200 Series). Prior to GPC analysis, the samples were dissolved in THF and injected into a Polymer Standards Service (PSS) Security 1200 system featuring Agilent HPLC vacuum degasser, isocratic pump, refractive index (RI) detector and UV detector (270 nm). Separation was achieved with four Waters Styragel columns (HR0.5, HR2, HR4, HR6). All calibration and analysis were performed at 30 ^{o}C using THF as the mobile phase (1.0 mL/min) with injection volumes of 20 uL. Data collection and processing were performed using PSS WinGPC Unity software. Molecular weights (M_n and M_w) were calculated against a standard polystyrene calibration curve.

Thermogravimetric (TGA) Analysis

TGA analysis was carried out on a TA Instruments (TGA Q500) using a nitrogen flow at a rate of 40 mL min^{-1}. Data was collected after placing about 10 mg of sample in a clean platinum pan. All samples were initially heated to 105 ^{o}C (heating rate of 10 ^{o}C min^{-1}) and kept isothermally for 20 minutes before heated to 600 ^{o}C at a heating rate of 10 ^{o}C min^{-1}.

Differential Scanning Calorimetry (DSC)

DSC was performed using a TA Instruments DSC Q100. All samples were dried at 40 ^{o}C for 24 h under vacuum prior to the DSC analysis. In a typical experiment, approximately 5 mg of sample was weighted directly in a DSC aluminum sample pan, which was then sealed by the lid of a pinhole by cold-pressing. An annealing procedure at a temperature lower than the sample's glass transition temperature was applied, *i.e.*, after loading into the TA-Q100, the sample was heated to 105 ^{o}C at a rate of 5 ^{o}C min^{-1} and kept isothermally for 40 minutes prior to being quenched to 30 ^{o}C with liquid nitrogen. Then, the DSC thermograms were recorded by increasing the temperature to 200 ^{o}C at a rate of 10 ^{o}C min^{-1}. The glass transition temperatures were calculated using a TA Universal Analysis software.

Contact Angle

Static contact angle measurements were conducted on a FTÅ200 Dynamic Contact Angle Analyzer (First Ten Ångstroms, USA) equipped with a B/W camera (Edmund Scientific). Sample films were prepared by dropping 5 mL aqueous suspension of samples (0.5 wt%) on glass slides (18 mm × 18 mm) and drying the glass slides at ambient environment and temperature for four days. The prepared films were placed onto a platform underneath a flat-tipped needle syringe and in front of camera. Contact angles were measured using 4 μL droplets of MilliQ water onto the film within 3 s at about 20 and 50 ^{o}C, respectively. After measurements, the films were further vacuum dried at 40 ^{o}C for 72 h to calculate the water content.

UV-vis Absorption and Fluorescence Spectroscopy

Uv-vis absorption spectra were measured using a Lambda 35 UV-vis spectrometer (Perkin Elmer). Fluorescence measurements were performed with a Shimadzu RF-5301PC equipped with a 150 W xenon lamp at about 20 °C and 50 °C, respectively. The widths of both the excitation slit and emission slit were set at 5.0 mm.

Results and Discussion

Initiator-Modified CNCs

CNCs, which bear numerous hydroxyl functional groups on the surface, were first esterified to introduce initiating sites for "graft-from" approach. The resultant product was then used as the AGET-ATRP agent for graft poly(NIPAAM-*co*-EANI), as illustrated in Scheme 1. The esterification reaction was conducted with excessive BiB to CNCs to improve the bromine content on the surface of CNCs. [35] Good dispersion of CNCs in solvent DMF (See supporting information, Figure S1) as reported [8] ensured homogeneous esterification in the surface of CNCs. The successful immobilization of initiator on CNCs was confirmed by FTIR (Figure 1). Compared to the FTIR spectrum of unmodified CNCs, the appearance of a carbonyl ester stretch vibration at 1725 cm^{-1} in the spectrum of CNC-Br provides the evidence of the covalent attachment of the initiator. There was no significant change in OH signal at 3350 cm^{-1}, indicating that a limited amount of surface OH groups was substituted and the internal OH groups remain untouched.

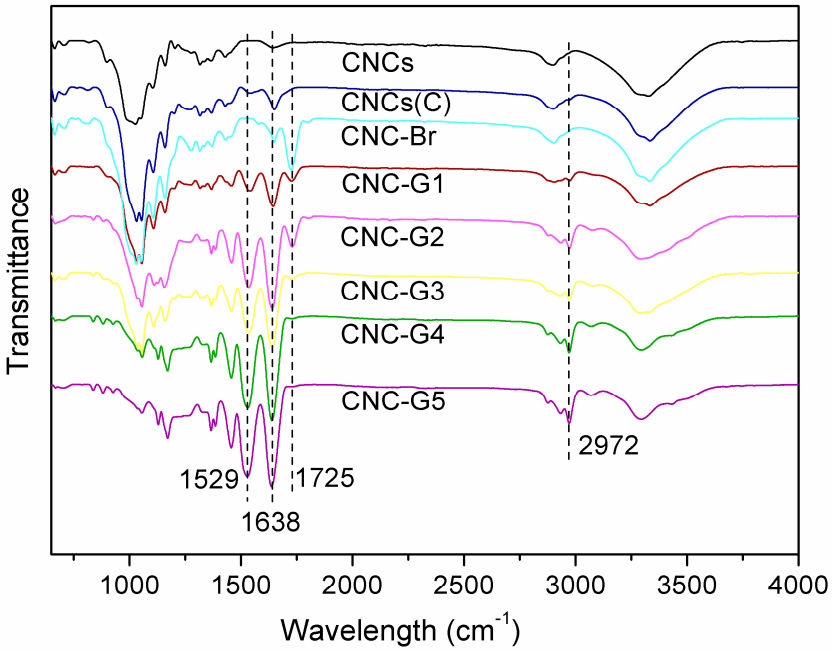

Fig. 1 FTIR spectra of unmodified CNCs, initiator-immobilized CNCs (CNC-Br) , surface-grafted CNCs and CNCs after cleavage of polymer brushes (CNCs(C)).

Solid-state ^{13}C NMR analysis was also used to determine the structure change after the initiator immobilization (Figure 2). The appearance of peaks at 172, 36, and 31 ppm for CNC-Br indicated that ester group was successfully on CNCs. In terms of bromine content, approximately 8 initiator site with Br was found for every 100 glucose units as obtained from the integral ratio at 172 and 105 ppm. The bromine content was calculated as 0.46 mmol/g based on the mass of CNC-Br (See Supporting Information, Equation (1)). To estimate the number of available initiator sites on the surface, a crude model of a nanocrystal developed by Huang et al. was adopted. [20] The bromine content of 0.46

mmol/g corresponds to 68.4 % initiator substitution of available surface glucose units. In addition, both CNCs and CNC-Br showed typical patterns of the native crystalline form of cellulose (cellulose I) in the range of 60-110 ppm. [44] The shoulder peaks for the C6 (63 ppm) and C4 (85 ppm) carbons were associated with amorphous and surface regions of CNCs. [19] The crystalline degree of CNC-Br, calculated from the integral ratio at the two peaks of C4 carbon, almost remained unchanged compared to that of CNCs (58% for CNC-Br and 55% for CNCs), [45] which indicated that the crystalline cores of the CNCs were not significantly affected by the esterification reaction while the modification was only limited on the surfaces of the nanocrystals.

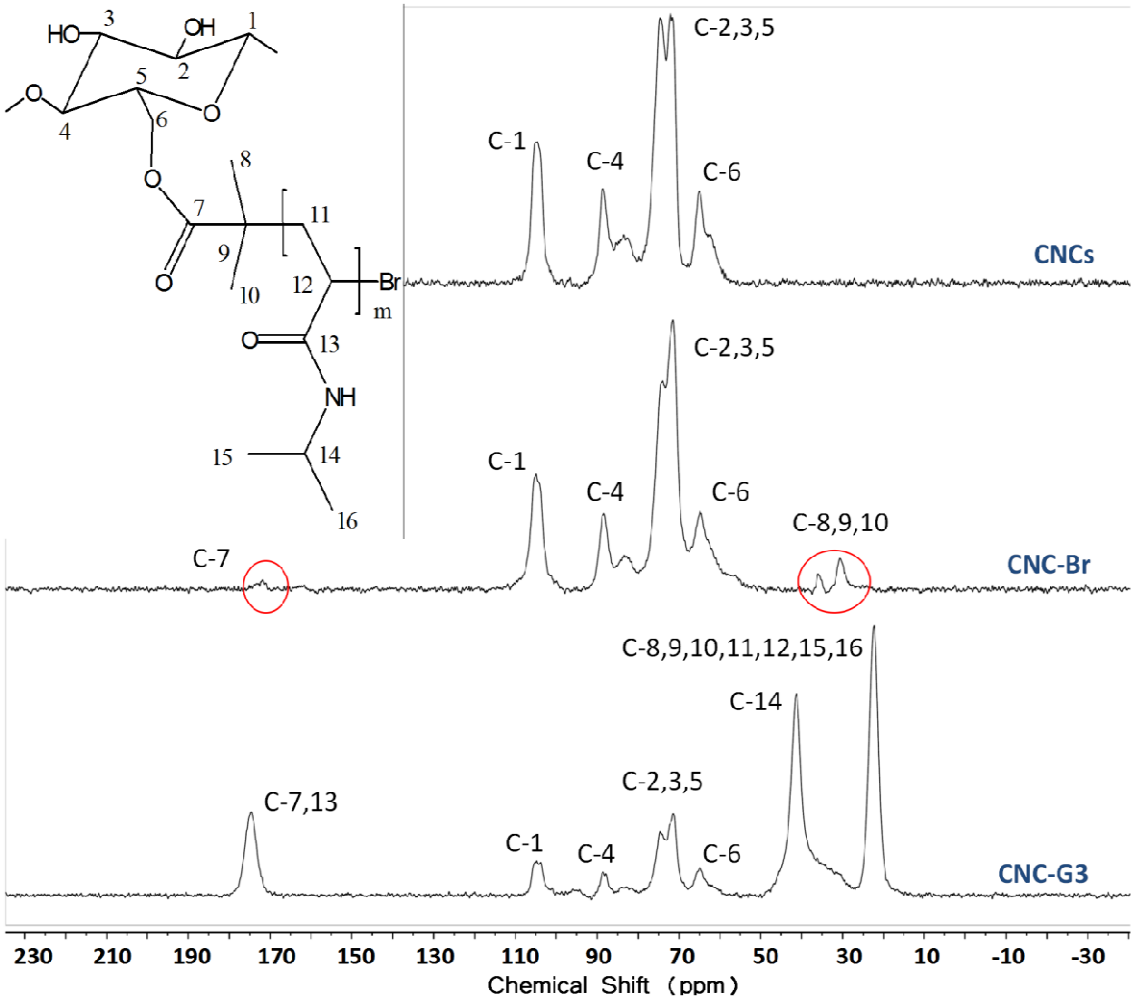

Fig. 2 Solid-state ^{13}C NMR spectra of unmodified CNCs, initiator-immobilized CNCs and representative surface-grafted CNCs (CNC-G3).

CNCs Grafted with Polymer Brushes

The obtained CNC-Br was used to graft PNIPAAM-*co*-PEANI brushes from the immobilized initiator on CNCs via SI-AGET-ATRP (step 2, Scheme 1). A series of surface-grafted CNCs were prepared with various volume ratios of CH_3OH and H_2O in the reaction system.

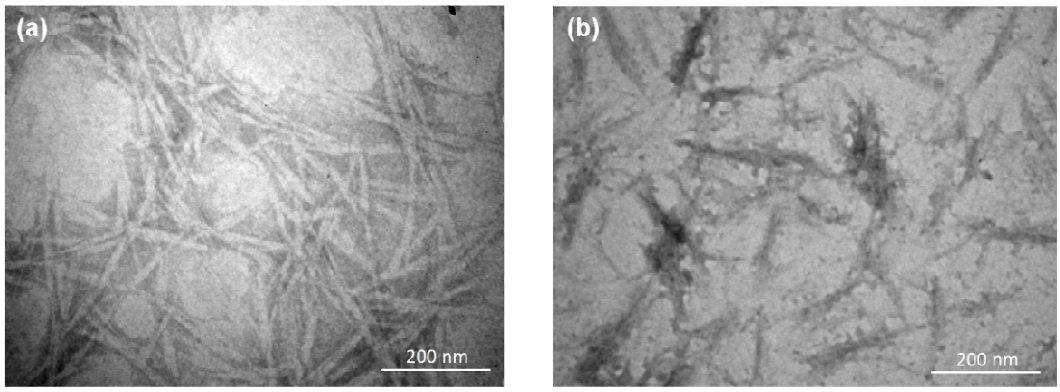

Fig. 3 TEM images of unmodified CNCs (a) and surface-grafted CNCs (b)

The morphology change of CNCs before and after modification was studied by TEM imaging, as shown in Figure 3. The obtained starting CNCs material were rod-like particles with the size of 5-15 nm in width and 100-200 nm in length, which are similar to the reported sizes of CNCs by sulfuric acid hydrolysis. [46] The surface-grafted CNCs observed became coarse and wide causing the rigid rod-like structure not as clear as unmodified CNCs. The change in the morphological integrity before and after grafting modification could be taken as indication of the presence of polymer brushes.

The differences between modified and unmodified CNCs were further determined and analyzed by FTIR and solid-state ^{13}C NMR. This series of surface-grafted CNCs displayed similar FTIR spectra, as shown in Figure 1. Successful surface grafting of PNIPAAM brushes on CNCs was evidenced by the appearance of new peaks at 1650 and 1546 cm^{-1} corresponding to the amide stretch and amine bend of PNIPAAM as well as the peak at 2972 cm^{-1} corresponding to C-H stretch of isopropyl. There was an increase in these peaks' intensity from CNC-G1 to CNC-G5, indicating that the thickness of

polymer brushes increase as the volume ratio of CH_3OH and H_2O decreases. FTIR spectrum of CNCs after cleavage of polymer brushes (CNCs(C)) is similar to that of unmodified CNCs (Figure 6). Very limited grafted PNIPAAM was detected verified a sufficient saponification reaction, and thus representative cleaved polymer chains. [26] It also suggested that no discernable changes in crystallinity or morphology took place during the esterification and subsequent grafting polymerization. In the solid-state ^{13}C NMR spectrum of CNC-G3 (Figure 2), the appearance of intense peak at 175, 41 and 22 ppm corresponding to PNIPAAM further support that PNIPAAM brushes were grafted onto the surface of CNCs [47] (No signal of dye groups was detected due to the low dosage of EANI). The patterns of CNC-G3 between 60 and 110 ppm were roughly the same as that of CNCs besides the relative signal intensity, indicating that the CNC core remains during the SI-AGET-ATRP process.

The thermal degradation behaviors of surface-grafted CNCs were investigated by TGA, as seen in Figure 4. TGA and derivative TGA curves dramatically changed after esterification and surface grafting. The thermal degradation behavior of the unmodified CNCs is comparable to that of sulfuric acid hydrolyzed bacterial celluloses (Table 1) [48] The significant decrease in the degradation temperature compared to native cellulose can be attributed to the high content of *in-situ* formed sulfate group on CNCs. [48] The further decrease in decomposition temperature of CNC-Br can be explained by the substitution of OH group by ester group, which has similar effect on the degradation behavior as

sulfate acid. The TGA curves trended toward high temperature direction and tended to be close to that of bulk PNIPAAM from CNC-G1 to CNC-G5. [49] Similarly, derivative TGA profiles of surface-grafted CNCs show two main peaks shifting to the higher temperature from CNC-G1 to CNC-G5. The shift of decomposition peaks and accompanying shape change indicated the increasing content of grafted PNIPAAM brushes.

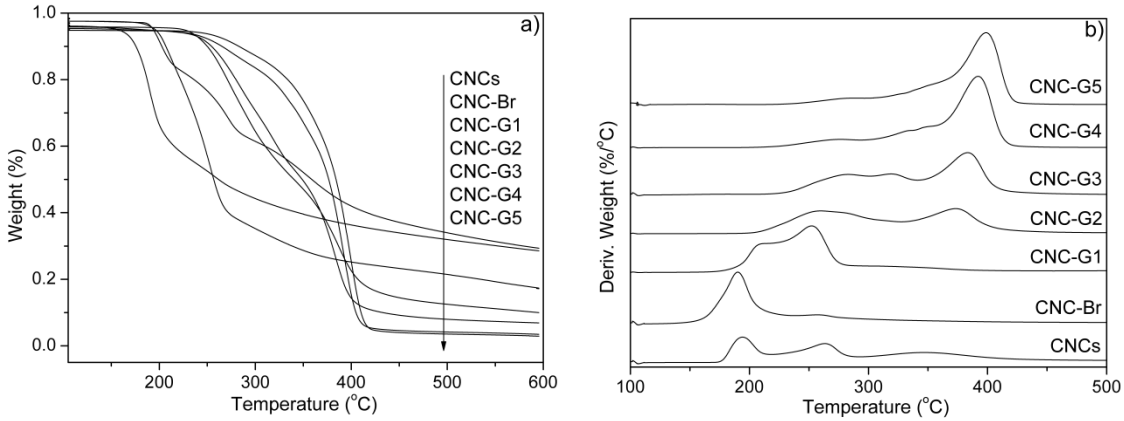

Fig. 4 Thermograms of unmodified CNCs, initiator-immobilized CNCs and surface-grafted CNCs. a) Weight loss (%) as a function of temperature; b) Derivative Weight loss (% °C) as a function of temperature.

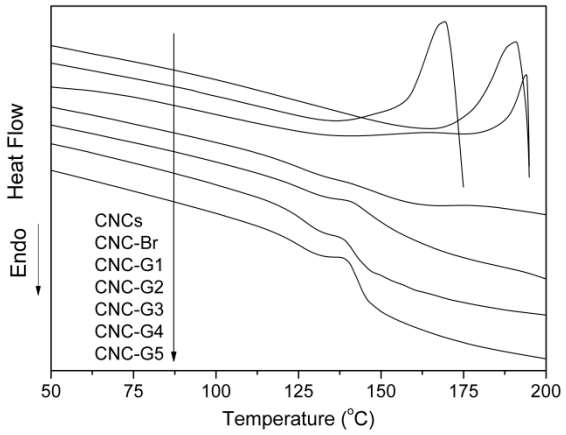

Fig. 5 DSC thermograms of unmodified CNCs, initiator-immobilized CNCs and surface-grafted CNCs

Table 1 Decomposition and glass transition temperatures of related CNC samples

Sample	CNCs	CNC-Br	CNC-G1	CNC-G2	CNC-G3	CNC-G4	CNC-G5
T_{onset} (°C)	183.6	175.0	212.0	229.3	250.5	270.7	278.0
$T_{max.}$ (°C)	194.3	190.2	252.3	373.3	383.3	392.0	394.8
T_g (°C)	-	-	-	146.7	145.2	143.6	141.6

T_{onset}: Onset decomposition temperature; T_{max}: Temperature at maximum decomposition rate; T_g: Glass transition temperature

Figure 5 illustrated DSC curves of CNCs before and after modification. No glass transition but only the onset of thermal degradation was observed for unmodified CNCs in differential scans due to their highly crystalline nature. CNC-Br shows similar

characteristic because of the limited esterification on the surface of CNCs. All surface-grafted CNCs except CNC-G1 showed a glass transition temperature in the range of 141-147 ^{o}C, which is higher than 130 ^{o}C, the reported glass transition temperature of amorphous PNIPAAM. [26] In addition, the glass transition of surface-grafted CNCs became more and more distinct and trended to be close to that of bulk PNIPAAM with an increase in the amount of polymer brushes present on CNCs. The increase in the glass transition temperature of surface-grafted CNCs can be explained by the restriction of the mobility of grafted PNIPAAM chains to the surface of CNCs. [26] It was consistent with the reported results that increasing entanglement density of PNIPAAM hindered the mobility of chain segments and thus led to an increase in glass transition temperature.[50] Here, the restriction of mobility was weakened as the proportion of CNC core to grafted polymers was reduced, thus, resulting in a decrease in the glass transition temperature from CNC-G2 to CNC-G5.

Surface-Initiated AGET ATRP from CNCs

CH_3OH/H_2O mixed solvent is a widely used solvent system to conduct ATRP polymerization of NIPAAM and copolymerization with various monomers under mild conditions because of the miscibility of CH_3OH and H_2O as well as their good solubility for NIPAAM. The addition of water has been reported to be able to enhance the ATRP polymerization.[51] However, there are also several factors associated with ATRP in

aqueous media that lead to poor control of polymerization, including the large ATRP equilibrium constant which increases the rate of chain termination, partial dissociation of the halide ion from deactivator complex which leads to inefficient deactivation of the propagating radicals, hydrolysis of the carbon−halogen bond which diminishes chain-end functionality, and partial dissociation of certain Cu(I)/L complexes. [52,53] To address these issues, appropriate proportion of water needs to be determined for the ATRP of NIPAAM. Here, grafting PNIPAAM-*co*-PEANI brushes onto CNCs via SI-AGET-ATRP was performed with various volume ratios of CH_3OH and H_2O at room temperature. The method of AGET-ATRP was chosen since its Cu(I) could be regenerated from Cu(II) catalyst so that the polymerization was actually conducted at a relatively low ratio of Cu(I):Cu(II), which can effectively reduced the radical concentration. It has been reported that the characterization of polymer brushes produced by heterogeneous ATRP can be carried out by using sacrificial initiator. [54] Herein, sacrificial initiator EBiB was used to figure out whether the molecular weight and polydispersity of grafted polymers were comparable to those of the free polymers. In addition, AsAc was used as reducing agent to generate Cu(I) from Cu(II) catalyst.

Table 2. Conversion, molecular weights, and polydispersities of free and grafted polymers during SI-AGET-ATRP

Sample[a]	C_m[b], %	C_p[c], %	$M_{n,w}$[d]	$M_{n,cp}$[e]	PDI_{cp}[e]	$M_{n,lmfp}$[f]	PDI_{lmfp}[f]	$M_{n,hmfp}$[g]	PDI_{hmfp}[g]
CNC-G1	3.0	1.2 (1.2, -[h])	740	-[h]	-[h]	675	1.42	18,261	1.53
CNC-G2	8.7	4.7 (3.9, 0.8)	2,066	1,768	1.42	906	1.50	36,658	1.58
CNC-G3	16.8	11.8 (10.1, 1.7)	5,112	5,322	1.86	1,960	1.47	75,091	1.64
CNC-G4	35.4	28.8 (26.3, 2.5)	13,071	13,307	1.93	2,687	1.41	109,570	1.89
CNC-G5	59.5	46.6 (43.8, 2.8)	21,669	19,759	1.75	3,727	1.51	126,120	1.68

[a] Experiments were conducted with [NIPAAM]: [EBiB]: [CNC-Br]: [$CuBr_2$]: [PMDETA]: [AsAc]: [EANI]=200: 1: 0.46: 2: 4: 1: 2, [CNC-Br] was the converted mole concentration of bromine; [b] Conversion of monomer calculated based on the residual monomer from ^{1}H NMR; [c] Conversion of monomer calculated based on the produced polymers which includes two parts: one is the grafted polymers (generated by CNC-Br) calculated from the increased weight (the first number in the bracket), the other is the free polymers (generated by EBiB) calculated from ^{1}H NMR (the second number in the brace); [d] Theoretical average molecular weight calculated from the weight of grafted polymers ; [e] GPC analysis of cleaved polymers (CP); [f] GPC analysis of the peak at low molecular weight of free polymer (LMFP); [g] GPC analysis of the peak at high molecular weight of free polymer (HMFP); [h] Too weak signal to be detected.

The mechanism of polymerization was studied through calculation of monomer conversion, gravimetric analysis, characterization of cleaved polymers and free polymers. Details of conversion, molecular weights, and polydispersities of free and grafted polymers are listed in Table 2. The monomer conversions (C_m) calculated based on residual monomer were comparable to those (C_p) calculated based on produced polymer for this series of surface-grafted CNCs. The value difference might be attributed to the weight loss during washing and the integral deviation of ^{1}H NMR data. The monomer conversion increased with an increase in the volume ratio of CH_3OH and H_2O, confirming the reported conclusion that water improves the polymerization activity for NIPAAM. The SI-AGET-ATRP stopped at extremely low conversion without the addition of water for CNC-G1. Highest conversion of about 50% was attained for CNC-G5 with CH_3OH/H_2O volume ratio of 1:2. It should be noted that the amount of free polymers was unexpectedly low compared to that of grafted polymers considering the dosage ratio of EBiB and CNC-Br. It was expected that the addition of EBiB in water could increase the amount of free polymer after the reaction. One of the possible explanations is that free polymers transfers from solution phase to the surface of CNCs through chain transfer reaction. Similar phenomena of chain transfer to polymer was observed in free-radical solution polymerization. [55] The complication of simultaneous heterogenous and homogenous polymerization was also investigated by GPC analysis of free polymers. There were two distinct peaks in the molar mass spectra, with one being

located at low molecular weight while the other located at high molecular weight (see Supporting Information, Figure S3). The two parts of low and high molecular weight were probably generated by normal chain growth and chain termination, respectively. The signal intensity ratio of the first and second peak increased from CNC-G1 to CNC-G5, indicating that the effect of chain termination was gradually limited when the proportion of H_2O in the component solvent rose. It is consistent with the variation tendency of monomer conversion as lower degree of chain termination leads to higher monomer conversion. Base on the assumption that all bromine sites were actively initialized and no consideration of dye groups in polymer chains, the average molecular weight ($M_{n,\,w}$) of grafted polymers can be calculated from the increased weight of CNCs after grafting polymerization (See Supporting Information, Equation (2)). For the selected sample CNC-G3, another molecular weight ($M_{n,\,s}$) was calculated as 3, 914 from solid-state ^{13}C NMR (Figure 2) with the integral ratio at 175 and 105 ppm (See Supporting Information, Equation (3)). The calculated $M_{n,\,w}$ and $M_{n,\,s}$ were comparable to the molecular weight ($M_{n,\,cp}$) of the cleaved polymers from the GPC analysis, indicating that all three applied methods to characterize the length of polymer brushes are feasible and reasonable. However, free polymers cannot be used as substitute to characterize grafted polymers as $M_{n,\,w}$ and $M_{n,\,cp}$ are not comparable to either $M_{n,\,lmfp}$ or $M_{n,\,hmfp}$. The big difference in the molecular weight might be attributed to the simultaneous homogeneous and heterogeneous polymerization, which led to unknown chain transfer

and termination. [56] In spite of the variation in the graft length, the grafted polymers of surface-grafted CNCs showed moderate polydispersity indices (PDI, ~1.93), which indicated that SI-AGET-ATRP with the simultaneous homogenous and heterogeneous process was controlled to some extent.

Wettability of Surface-grafted CNCs

PNIPAAM is one of the most used thermo-responsive polymers as it exhibits a reversible phase transition in aqueous solution ranging between 30 and 35 ^{o}C (lower critical solution temperature, LCST), depending on its detailed molecular architecture.[36] Here, the thermo-responsiveness of surface-grafted CNCs was evaluated by contact angle measurements at temperature below and above the LCST of PNIPAAM. Contact angle measurements were repeatedly conducted in order to obtain average values and reduce measurement error, as presented in Table 3. Smooth film was attained for unmodified CNCs and contact angles were easily determined as 26 ° at 20 ^{o}C. In spite of the formation of rough surface with pores, the contact angle of CNC-Br film rose up to 82 ° because of the hydrophobic ester group covering the surface of CNCs. Both CNCs and CNC-Br showed no thermo-responsiveness upon temperature change from 20 to 50 ^{o}C, which corresponds to previously reported conclusion. [30,35] The surface-grafted CNCs showed big differences in film-forming ability due to the different content of grafted polymers. CNC-G1, CNC-G2 and CNC-G3 with relatively low content of polymer

brushes can only form rough films with cracks and pores. Contact angle of CNC-G2 and CNC-G3 cannot be detected as the water droplet spreads immediately. Considering that contact angle could be affected by the chemical composition of the surface and also the surface roughness, the failure of contact angle measurements can be due to the capillary action of the cracks and pores on the film. The exception of measured contact angle of CNC-G1 was attributed to the residual hydrophobicity of ester group on the surface owing to low grafting efficiency. No obvious temperature dependence of wettability was observed for CNC-G1. By comparison, CNC-G4 and CNC-G5 have good film-forming ability. Both of them exhibited apparent increase in contact angles with temperature shift from 20 to 50 ^{o}C, indicating that they possess thermo-responsiveness. Obviously, it is the grafted PNIPAAM brushes that caused variations in the wettability of surface-grafted CNCs in response to temperature change.[57] During the measurements of contact angle, both retained moisture in the film (~20%) and the water droplets contacted on the surface contribute to create the water environment for PNIPAAM brushes. Below LCST (20 ^{o}C), the brushes assume to be a stretched conformation as a result of intermolecular hydrogen bonding with water, resulting in a hydrophilic behavior. However, above LCST (50 ^{o}C), the brushes underwent a phase transition due to intramolecular hydrogen bonding, resulting in a collapsed brush conformation and more hydrophobic surface. [58]

Table 3. Contact Angles for Surface-Grafted CNCs below and above LCST

	CNCs	CNC-Br	CNC-G1	CNC-G2	CNC-G3	CNC-G4	CNC-G5
20 ^{o}C	26	82	37	-	-	46	50
50 ^{o}C	27	80	39	-	-	56	63

Thermo-Responsive Fluorescence of Surface-Grafted CNCs

The resulting surface-grafted CNCs were thoroughly washed until no absorption of supernatant at 375 nm was detected to remove unpolymerized EANI that might be adsorbed on the surface. The absorption peak at 375 nm of surface-grafted CNCs, which was comparable to that of EANI (Figure 6), indicated that dye monomer were covalently encapsulated into the polymer brushes via copolymerization. The successful covalent embedment of dye groups was also verified by the exhibiting fluorescence emission associated with EANI when a suspension of surface-grafted CNCs was illuminated at 365 nm (Figure 7). Here, the CNCs grafted with PNIPAAM-*co*-PEANI were expected to possess thermo-responsive fluorescence based on the thermo-responsiveness of PNIPAAM. The fluorescence of surface-grafted CNCs in aqueous suspensions was determined by measuring the emission intensities under the excitation of 375 nm at 20 and 50 °C, as presented in Figure 8. When temperature is changed from 20 to 50 °C, all surface-grafted CNCs showed an increase in fluorescent intensity, which was contrary to that of pure EANI solution. In addition, both the fluorescent intensity and sensitivity to

temperature were enhanced in the case of CNCs grafted with thick polymer brushes. Considering the fact that increasing temperature enhances non-radiative transition and reduces fluorescence quantum efficiency of dyes, [59,60] the abnormal change of fluorescent intensity with temperature variation could be attributed to the thermo-responsiveness of PNIPAAM brushes, which altered the surrounding environment of dye groups. As discussed above, PNIPAAM brushes underwent a structural transition from stretched conformation to collapsed conformation due to thermal-driven chain dehydration with temperature changing from below LCST to above LCST, resulting in the reduction of hydrophilicity (Figure 9). There are two main factors contributing to the enhanced fluorescence of surface-grafted CNCs above LCST: One is the increased hydrophobicity of the surrounding environment for dye groups, which reduces the solvent effect of polar water and consequently leads to an increase in the fluorescence quantum efficiency; the other is the collapsed and shrunk conformation, which inhibits the rotation and vibration of dye groups and decreases the nonradiative transition. The intelligent nature makes these surface-grafted CNCs potential drug carriers in biomedical area. The combination of fluorescence and thermo-responsiveness further enable the use of fluorescence techniques to study the cellular uptake of CNCs, biodistribution of CNCs in vivo and the drug release process of CNC carriers.

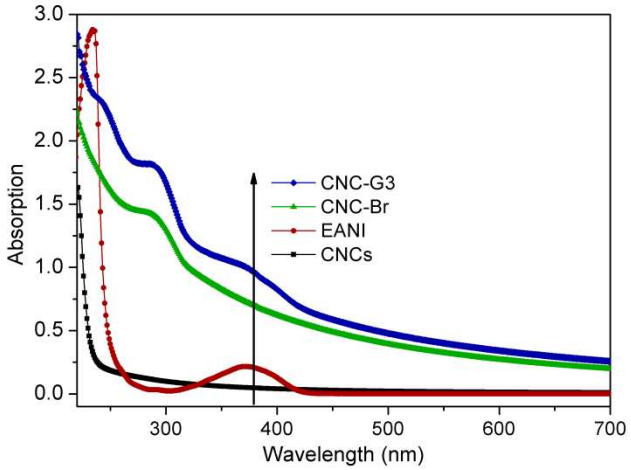

Fig. 6 UV-vis spectra of CNC (0.1 wt% in H_2O), CNC-Br (0.1 wt% in H_2O), CNC-G3 (0.1 wt% in H_2O) and EANI (5×10^{-6} M in H_2O)

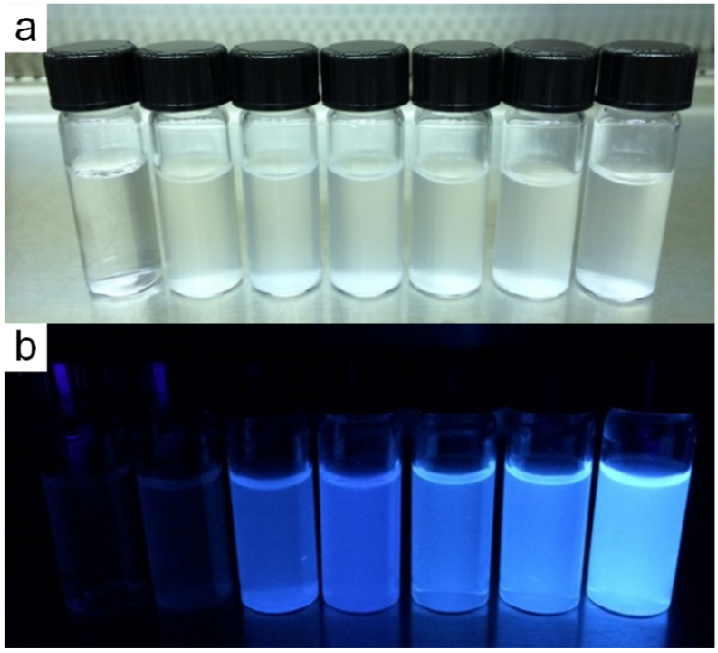

Fig. 7 Photographs of CNC suspensions (0.05 %) under sunlight (a) and 365-nm UV illumination (b).The samples are CNCs, CNC-Br, CNC-G1, CNC-G2, CNC-G3, CNC-G4, and CNC-G5 from left to right, respectively.

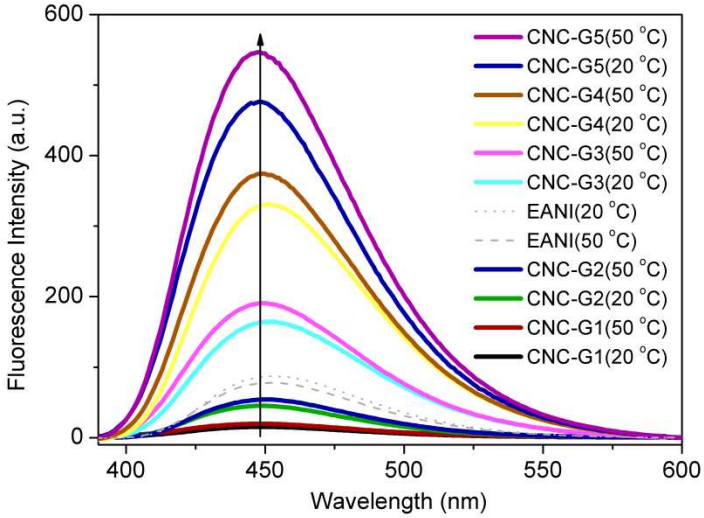

Fig. 8 Fluorescence emission spectroscopy of surface-grafted CNCs (0.02 wt% in H_2O) and EANI (10^{-6} M in H_2O)

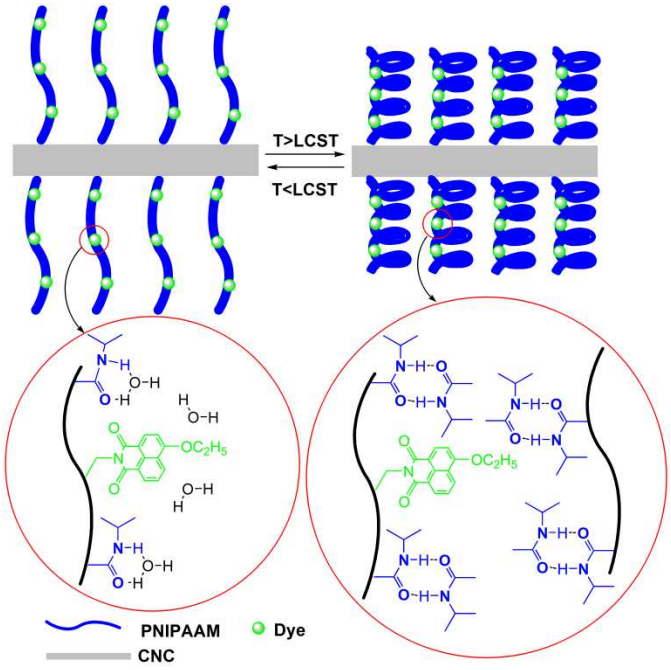

Fig. 9 Conformation of grafted PNIPAAM brushes below LCST and above LCST

Conclusions

Polymer-grafted CNCs with fluorescence and thermo-responsiveness were obtained via SI-AGET-ATRP under various volume ratios of CH_3OH and H_2O. The monomer conversion and molecular weight of polymer brushes increased as the volume ratio of CH_3OH and H_2O decreased. There was a big difference between the molecular weight of free and grafted polymers. A large scale of chain transfer from solution to the surface of CNCs occurred in the presence of simultaneous homogeneous and heterogeneous polymerizations. Based on the thermo-responsiveness of PNIPAAM, CNCs grafted with Poly(NIPAAM-*co*-EANI) showed thermo-enhanced fluorescence, which was contrary to that of pure dye solution. The presented results illustrated the usefulness of this synthetic

strategy applied in this paper to turn CNCs into novel multifunctional nanomaterials, which would open up for possible biomedical applications as drug carriers, fluorescent probes and sensors.

Acknowledgements

The support of this work by the National Natural Science Foundation of China (No.31200453, No.31300483), Natural Science Foundation of Jiangsu Province of China (No. BK20130971), the Priority Academic Program Development of Jiangsu Higher Education Institutions (PAPD) and Jiangsu Provincial Government Scholarship for Overseas Studies is gratefully acknowledged.

Notes and references

[a] *Jiangsu Provincial Key Lab of Pulp & Paper Science & Technology, Nanjing Forestry University, 159 Longpan Road, Nanjing 210037, China*

[b] *Renewable Bioproducts Institute, Georgia Institute of Technology, 500 10th St NW, Atlanta, GA 30332, United States. E-mail: yulin.deng@ipst.gatech.edu; Tel: +1 404 894 5759*

[c] *School of Pulp and Paper Making, Hubei University of Technology, Wuhan 430068, China,*

[d] *College of Materials and Engineering, Nanjing Forestry University, 159 Longpan Road, Nanjing 210037, China*

† Electronic Supplementary Information (ESI) available: [Synthesis of EANI, TEM image of CNCs from suspension in DMF, typical ^{1}H NMR spectra of the supernatant after SI-AGET-ATRP, molecular weight distributions of free polymer, and contact angle pictures of surface-grafted CNCs]. See DOI:

1 K. K. Jain, *Drug Discov. Today,* 2005, **10**, 1435-1442.

2 S. Baruah, J. Dutta, *Environmen. Chem. Lett*, 2009, 7, 191-204.

3 J. R. McKee, S. Hietala, J. Seitsonen, J. Laine, E. Kontturi, O. Ikkala, *ACS Macro Lett*., 2014, **3**, 266-270.

4 X. Wang, L.-H. Liu, O. Ramström, M. Yan, Exp. Bio. Med., 2009, 234, 1128-1139.

5 Y. Habibi, L. A. Lucia, O. J. Rojas, *Chem. Rev.,* 2010, **110**, 3479-3500.

6 D. Klemm, F. Kramer, S. Moritz, T. Lindström, M. Ankerfors, D. Gray, A. Dorris, *Angew. Chem.Int. Edit,* 2011, **50**, 5438-5466.

7 R. J. Moon, A. Martini, J. Nairn, J. Simonsen, J. Youngblood, *Chem. Soc. Rev.,* 2011, **40**, 3941-3994.

8 M. A. S. Azizi Samir, F. Alloin, A. Dufresne, *Biomacromolecules,* 2005, **6**, 612-626.

9 B. Braun, J. R. Dorgan, *Biomacromolecules,* 2008, **10**, 334-341.

10 Y. Habibi, H. Chanzy, M. R. Vignon, *Cellulose,* 2006, **13**, 679-687.

11 M. Hasani, E. D. Cranston, G. Westman, D. G. Gray, *Soft Matter,* 2008, **4**, 2238-2244.

12 C.Goussé, H.Chanzy, G.Excoffier, L. Soubeyrand, E.Fleury, *Polymer,* 2002, **43**, 2645-2651.

13 G. Siqueira, J. Bras, A.Dufresne, *Biomacromolecules,* 2008, **10**, 425-432.

14 A. Junior de Menezes, G. Siqueira, A. A. Curvelo, A. Dufresne, *Polymer,* 2009, **50**, 4552-4563.

15 J. Pandey, W. Chu, C. Kim, C. Lee, S. Ahn, *Composit. Part B: Eng.,* 2009, **40**, 676-680.

16 E. Kloser, D. G. Gray, *Langmuir,* 2010, **26**, 13450-13456.

17 L. JunkeráNielsen, *Chem. Commun.,* 2010, **46**, 8929-8931.
18 K. A. Mahmoud, J. A. Mena, K. B. Male, S. Hrapovic, A. Kamen, J. H. Luong, *ACS Appl. Mater. Inter.,* 2010, **2**, 2924-2932.
19 T. Abitbol, A. Palermo, J. M. Moran-Mirabal, E. D. Cranston, *Biomacromolecules,* 2013, **14**, 3278-3284.
20 J.-L. Huang, C.-J. Li, D. G. Gray, *ACS Sustain. Chem. Eng.,* 2013, **1**, 1160-1164.
21 S. Dong, M. Roman, *J. Am. Chem. Soc.,* 2007, **129**, 13810-13811.
22 Y. N. Liu, H. Y. Yu, Z. Y. Qin, L. Chen, *Adv. Mater. Res.,* 2012, **557**, 563-566.
23 F. Azzam, L. Heux, J.-L. Putaux, B. Jean, *Biomacromolecules,* 2010, **11**, 3652-3659.
24 A. P. Mangalam, J. Simonsen, A. S. Benight, Biomacromolecules, 2009, 10, 497-504.
25 T. Sato, M. M. Ali, R. Pelton, E. D. Cranston, *Biomacromolecules*, 2012, **13**, 3173-3180.
26 J. O. Zoppe, Y. Habibi, O. J. Rojas, R. A. Venditti, L.-S. Johansson, K. Efimenko, M. Österberg, J. Laine, Biomacromolecules, 2010, 11, 2683-2691.
27 J. O. Zoppe, M. Osterberg, R. A. Venditti, J. Laine, O. J. Rojas, *Biomacromolecules,* 2011, **12**, 2788-2796.
28 J. O. Zoppe, R. A. Venditti, O. J. Rojas, *J. Colloid and Interf Sci.,* 2012, **369**, 202-209.
29 J. Yi, Q. Xu, X. Zhang, H. Zhang, *Cellulose,* 2009, **16**, 989-997.
30 K. H. Kan, J. Li, K. Wijesekera, E. D. Cranston, *Biomacromolecules,* 2013, **14**, 3130-3139.
31 K. Matyjaszewski, J. Xia, *Chem. Rev.,* 2001, **101**, 2921-2990.
32 K. Matyjaszewski, N. V. Tsarevsky, *Nat. chem.,* 2009, **1**, 276-288.
33 S. Edmondson, V. L. Osborne, W. T. Huck, *Chem. Soci. Rev.,* 2004, **33**, 14-22.
34 J. Yi, Q. Xu, X. Zhang, H. Zhang, *Polymer,* 2008, **49**, 4406-4412.
35 G. Morandi, L. Heath, W. Thielemans, *Langmuir,* 2009, **25**, 8280-8286.
36 G. Morandi, W. Thielemans, *Polym. Chem.,* 2012, **3**, 1402-1407.
37 H. Rosilo, J. R. McKee, E. Kontturi, T. Koho, V. P. Hytönen, O. Ikkala, M. A. Kostiainen, *Nanoscale*, 2014, **6**, 11871-11881
38 W. Jakubowski, K. Matyjaszewski, *Macromolecules,* 2005, **38**, 4139-4146.
39 H. Schild, *Prog. Polym. Sci,* 1992, **17**, 163-249.
40 A. Matsuyama, F. Tanaka, *Phys. Rev. lett.,* 1990, **65**, 341-344.
41 I. Grabtchev, T. Konstantinov, S. Guittonneau, P. Meallier, *Dyes Pigments,* 1997, **35**, 361-366.

42 I. Grabchev, T. Konstantinova, *Dyes Pigments,* 1997, **33**, 197-203.
43 S. Beck-Candanedo, M. Roman, D. G. Gray, *Biomacromolecules,* 2005, **6**, 1048-1054.
44 R. Atalla, D. L. VanderHart, *Solid State Nucl. Mag.,* 1999, **15**, 1-19.
45 S. Park, D. K. Johnson, C. I. Ishizawa, P. A. Parilla, M. F. Davis, *Cellulose,* 2009, **16**, 641-647.
46 J. Majoinen, A. Walther, J. R. McKee, E. Kontturi, V. Aseyev, J. M. Malho, J. Ruokolainen, O. Ikkala, *Biomacromolecules*, 2011, **12**, 2997-3006.
47 P. W. Chung, R. Kumar, M. Pruski, V. S. Y. Lin, *Adv. Funct. Mater.,* 2008, **18**, 1390-1398.
48 M. Roman, W. T. Winter, *Biomacromolecules,* 2004, **5**, 1671-1677.
49 S. Ifuku, J. F. Kadla, *Biomacromolecules,* 2008, **9**, 3308-3313.
50 W. Yin, H. Yang, R. Cheng, *Eur. Phys.J. E,* 2005, **17**, 1-5.
51 G. Masci, L. Giacomelli, V. Crescenzi, *Macromol. Rapid Comm.,* 2004, **25**, 559-564.
52 A. Simakova, S. E. Averick, D. Konkolewicz, K. Matyjaszewski, *Macromolecules,* 2012, **45**, 6371-6379.
53 N. V. Tsarevsky, T. Pintauer, K. Matyjaszewski, *Macromolecules,* 2004, **37**, 9768-9778.
54 S. Hansson, E. Ostmark, A. Carlmark, E. Malmström, *ACS Appl. Mater. Inter.,* 2009, **1**, 2651-2659.
55 N. M. Ahmad, Frank Heatley, P. A. Lovell, *Macromolecules*, 1998, **31**, 2822-2827.
56 W. A. Braunecker, N. V. Tsarevsky, A. Gennaro, K. Matyjaszewski, *Macromolecules,* 2009, **42**, 6348-6360.
57 J. Lindqvist, D. Nyström, E. Östmark, P. Antoni, A. Carlmark, M. Johansson, A. Hult, E. Malmström, *Biomacromolecules,* 2008, **9**, 2139-2145.
58 T. Sun, G. Wang, L. Feng, B. Liu, Y. Ma, L. Jiang, D. Zhu, *Angew. Chem. Int. Edit.,* 2004, **43**, 357-360.
59 R. F. Kubin, A. N. Fletcher, *J. Lumin.,* 1983, **27**, 455-462.
60 E. P. Kirby, R. F. Steiner, *J. Phys. Chem.,* 1970, **74**, 4480-4490.

Graphical Abstract

Fluorescent and thermo-responsive polymer grafted cellulose nanocrystals (CNCs) were prepared via surface-initiated activators generated by electron transfer for atom transfer radical polymerization (SI-AGET-ATRP). The length of grafted polymer brushes could be tuned by changing the water proportion of CH_3OH/H_2O two-component solvent system. The obtained surface-grafted CNCs showed thermo-enhanced fluorescence owing to the thermal-driven chain dehydration of the grafted PNIPAAM brushes.